Chapter 6

The Nucleus of Comet Hyakutake C/1996 B2

6.1 Background

Six months after the discovery of Hale-Bopp, a Japanese amateur astronomer discovered his second long-period comet in a seven-week period, an 11th magnitude smudge (Nakamura and Nakano 1996). Four days later it was realized that this comet would make a very close approach to Earth in late March and probably be an easy naked-eye object (Marsden 1996). The rest of the story is well known: comet Hyakutake blazed through the Northern Hemisphere sky at a visual magnitude of about 0 and sported a tail extending many tens of degrees. The photograph in Fig. 6.1 shows how the comet looked to my camera on 25 Mar 1996; the field of view is about 40 degrees wide. In contrast to Hale-Bopp later on, Hyakutake flashed in and out of our skies in a week. The short lead time necessitated a scramble for requesting access to telescopes; fortunately many observatory directors recognized the special significance of this comet – the closest one to Earth since 1983 and the brightest one since 1976 – for which comet scientists were exceedingly grateful.

6.2 Thermal Measurements

A track of observations was done at the Very Large Array (VLA), two days after the March 25th close approach of the comet. I have described that experiment elsewhere (Fernández *et al.* 1997a) and I reproduce much of the text here. Our infrared thermal data were obtained around the time of the comet's close approach, and have been described in detail by Lisse *et al.* (1999b). Since most of the work in that wavelength regime for this comet was done by Lisse, I will give space to those results only as they relate to my data.

6.2.1 Details of Observations

Our VLA observations consisted of one twelve-hour track from 0700 UT to 1900 UT on 27 March, 1996. The flux calibrator was 3C 286 (QSO J1331+3030, flux of about 5.2 Jy), and our phase calibrator was 4C 76.03 (a radio galaxy having a flux of about 2.2 Jy) (Perley and Taylor 1996). Individual integrations were ten seconds long; the total amount of time spent integrating on the comet was about ten hours. Phase stability during the track was good.

During the observation, the comet itself was between 0.121 and 0.131 AU from Earth, 1.00 and 0.989 AU from the Sun, and the phase angle was between 85.7° and 90.2°. The ephemeris that was used at the time of the observation was provided by D. K. Yeomans (private communication), but, owing to the proximity of the comet, had formal positional uncertainties of 8 arcsec in right ascension and 2 arcsec in

Figure 6.1: Comet Hyakutake in a 40°-wide field of view. This is a photograph of the comet taken by me near the time of closest approach on 25 Mar 1997. The field of view on the long dimension is about 40 degrees; the tail is clearly visible over most of that arc.

declination (1-σ). The proper motion of the comet ranged from 4.7 to 5.5 arcsec per integration-time, and decreased by about 0.065 arcsec per integration-time per hour.

The VLA telescopes can only track the linear proper motion of a source. But, due to the rapid motion of the comet, we had to take into account the second order motion. We updated the linear tracking rates every 3 to $3\frac{1}{2}$ minutes so that the array was always pointed within one synthesized beam (3.5 arcsec) of the most accurate formal position of the comet available at the time.

6.2.2 Data Reduction and Correction

The standard data reduction yielded no significant signal from the comet. One problem we considered was that, due to the positional uncertainty of the comet, the signal might have been smeared during the course of our observation. A more accurate ephemeris of the comet, produced by D. K. Yeomans a few weeks after perigee, revealed that our tracking rates were not significantly in error (off by ≤ 0.01 arcsec per integration time), but the center of pointing was indeed offset from the true position of the comet by up to 6.6 arcsec at times during our observing run. It should be pointed out here that the half-power bandwidth (HPBW) of the VLA telescopes at our observing frequency is 5.3 arcmin and primary beam attenuation is negligible for these offsets. In essence, the amplitude and phase of the complex integration data points were correct, but the projected baselines (or uv-spacings) of the telescopes were slightly offset, because of the difference in the observed and actual position of the comet. We recalculated the correct uv-spacings for each baseline for every ten-second integration, and inserted these corrected spacings into the dataset. After the correction, we obtained a more robust map.

This problem is important to consider for any interferometric observation of a fast-moving object, because of the inherent uncertainty in the ephemeris and in the way the data are taken at the observatory. To stress this latter point, it was important that, in order to correctly reduce our data, we understand intimately where the telescopes point at a given time, and what information pertaining to that are stored as "data." In this case the "data" were not correct, and we were forced to alter them by hand. Since the VLA (or any radio interferometric array) typically does not perform observations of this sort, we emphasize the special requirements of the data analyst in this situation. A description of some of the problems with interferometric observations of close, fast objects is given by de Pater *et al.* (1994).

Our CLEAN map, with 2- and 3-σ contours, is shown in Fig. 6.2. Since we had directly manipulated the data (via the corrections), we would expect the signature from the comet to appear in the middle of the map. The synthesized beam – 3.5 arcsec wide – is shown in the lower left. The field of view in this map is 4.2 arcmin by 4.2 arcmin, slightly smaller than the HPBW of the telescopes' primary beam. With such a synthesized-beam size, the nucleus would have appeared as a point source. The r.m.s. noise in our map is 7.6 μJy/beam.

There appear to be some linear structures or streaks running generally north-east to southwest in the map. These may be extended background sources passing through the field of view as the array tracked the comet, or indicative of a few

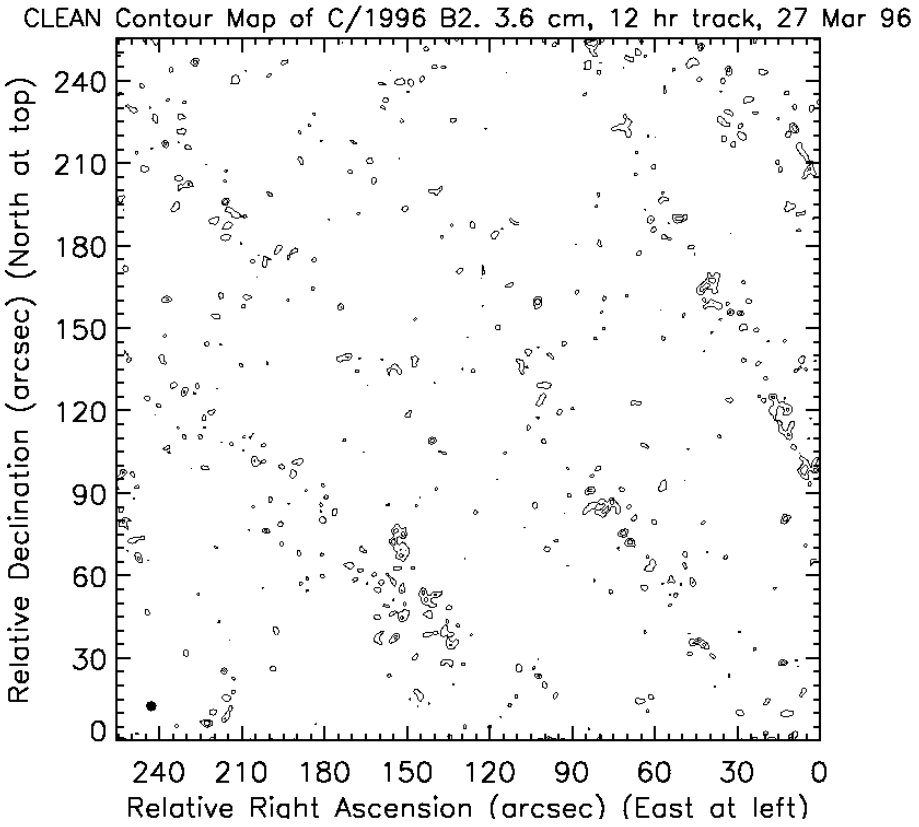

Figure 6.2: CLEAN contour map of C/1996 B2. This is acutally the CLEAN contour map of the field of view containing the comet, since we did not detect the object at the 3-σ level. We used the VLA on 27 Mar 1996 to generate this image, and the synthesized beam is the black dot at lower left.

anomalous visibility-data points. It is important to stress, however, that the structures appear only on the 1- and 2-σ level, and as such are not statistically significant. A histogram of pixel values is well-described by a Gaussian of $\sigma = 7.6$ μJy and shows no excess of pixels 1- or 2-σ from the mean. In addition, the structures have a low intensity. Integrating over the roughly $\sim 10^{2.5}$ synthesized-beams that they cover, the flux density is about 1 to 10 mJy. Had the hypothetical structures been tracked, they would have covered around 30 to 100 synthesized beams, based on the thickness of the streak. This implies their surface brightness was only $\sim$ 10 to 100 μJy/beam.

6.2.3 Implications for the Nucleus

Our measurement of the r.m.s. flux in the synthesized beam from the comet allows us to place a 3-σ upper limit on the thermal microwave continuum flux of 22.8 μJy at 3.55 cm. Of the six interferometric observations of a comet's microwave continuum, five (including Hyakutake) are upper limits. Our Hale-Bopp observations (Chapter 4) resulted in the only detection. Our Hyakutake upper limit is smaller than the other four: comet Austin (C/1982 M1 = 1982g = 1982 VI) was observed at 6 cm (Snyder *et al.* 1983) with an upper limit of 140 μJy; comet *IRAS*-Araki-Alcock (C/1983 H1 = 1983d = 1983 VII) was observed at 2 and 6 cm (de Pater *et al.* 1985) with upper limits of 750 and 90 μJy, respectively; comet Crommelin (27P = 1983n = 1984 IV) was observed at 2 cm (Schenewerk *et al.* 1986) with an upper limit of 136 μJy; and comet Halley (1P/1982 U1 = 1982i = 1986 III) was observed at 2 cm (Hoban and Baum 1987) with an upper limit of 100 μJy.

As mentioned in Chapter 3, it is not obvious which thermal model is the most applicable. The rotation period is about 6.3 hr (see next section), which would put the thermophysical parameter Θ close to unity for lunar-like thermal inertia. However, since the microwave data sample colder, subsurface layers, the ILM or even an isothermal model is probably more applicable. Also the high activity of the nucleus – approximately 50% of the surface is active (Lisse *et al.* 1999b) – probably helps to keep the insolation energy from penetrating deep below the surface, since much of it is being used to sublimate ice. Since we do not have information on the shape of the nucleus and since there does not yet seem to be a comprehensive model of the nucleus' rotation state, we will simplify matters by calculating an upper limit to the nucleus' radius by assuming the subsurface layer that we have sampled is isothermal.

To obtain an estimate of the nuclear size, we use

$$S_\lambda = \frac{2\pi kT}{\lambda^2}\epsilon_\lambda \frac{R^2}{\Delta^2}, \tag{6.1}$$

where S_λ is the measured flux density from the nucleus ($\leq$22.8 μJy), λ is the wavelength (3.55 cm), Δ is the geocentric distance (averaging 0.126 AU during the observation), k is the Boltzmann constant, T is the nuclear temperature, ϵ_λ is the emissivity at 3.55 cm, and R is the nucleus' effective radius.

Radar measurements of cometary nuclei have indicated that the microwave albedo is quite low, a few percent (Campbell *et al.* 1989). Thus, the emissivity of the nuclei is probably around 0.95, assuming that the emissivity is close to one

minus the albedo. For comparison, the emissivity of NEAs is roughly as high, 0.8 to 0.9 (Goldstein *et al.* 1984). The temperature is more problematical, but based on our efforts for Hale-Bopp (in Chapter 4), a temperature of 150 K for the sampled layer in Hyakutake's nucleus is not unreasonable. The extreme limits to the temperature range from about 300 or 350 K (for a very conductive nucleus) down to roughly 50 K (roughly the temperature of formation in the Kuiper Belt [Rickman 1991]).

We have combined all of this information into Fig. 6.3. Effective radius is plotted vs. temperature, with the solid curves representing four possible emissivities. The dotted line marks the temperature of an isothermal blackbody at the heliocentric distance, and the dashed line marks the approximate sublimation temperature for water ice. For the true emissivity and observed temperature of the nucleus, the radius could lie anywhere to the left of the appropriate point. For $\epsilon = 0.9$ and $T = 150$ K, the 3-σ upper limit to the radius is 3.0 km. This is consistent with our result obtained from the thermal-IR imaging (Lisse *et al.* 1999b), 2.4 ± 0.5 km, as well as the radar results by Harmon *et al.* (1997), 1.5 ± 0.5 km. Our estimate of the radius is not very sensitive to the temperature when $T \sim 200$ to 300 K, but it becomes 5 km for the 50 K limit.

6.2.4 The X-ray Connection

Our observations were simultaneous with many of the *ROSAT* observations of Hyakutake that occurred a few days after perigee (Lisse *et al.* 1996). Since non-thermal radio emission is frequently coincident with X-ray emission from other astrophysical sources, we were motivated to place an upper limit on the microwave emission from the location of the X-rays in Hyakutake's coma; the VLA field of view overlaps a portion of the X-ray emitting region reported by Lisse *et al.* (1996). The center of brightness of the X-ray emission with respect to the nucleus is about $2'$ north and $2\frac{1}{2}'$ east of the nuclear position (on 27.7 March UT), whereas our map extends only $2.1'$ from the nucleus. If we approximate the size of the X-ray emitting region as a $4'$-by-$8'$ oval, with the short axis on the Sun-comet line, then the overlap between the VLA field of view and the X-ray emitting region is a wedge that contains about 9% of the total X-ray flux, and about 13% of the total VLA field of view. Assuming the microwave flux from the coma follows the same spatial distribution as the X-ray flux, we calculate that the 3-σ upper limit to the microwave flux from the X-ray emitting region is 223 mJy. This value is more than a factor of two lower than that reported by Minter and Langston (1996), using the same-size X-ray emitting region of the coma. This result indicates that the mechanism responsible for the production of X-rays is not able to produce much microwave radiation. Lisse *et al.* (1996) found an X-ray luminosity of 4×10^{15} erg/s from the coma as measured by the *ROSAT* HRI, which is sensitive to 0.1- to 2.0-keV photons. Assuming a power law spectrum, where the intensity is proportional to $\nu^{-\alpha}$ (where ν is the frequency and α is the spectral index), and using the largest possible effective bandpass (1.9 keV) and our microwave upper limit, we find that α must be less (i.e., flatter) than 0.59, fairly flat. Some of the mechanisms postulated by Lisse *et al.* (1996) to explain the X-ray emission (e.g., magnetic field-line reconnection and magnetospheric

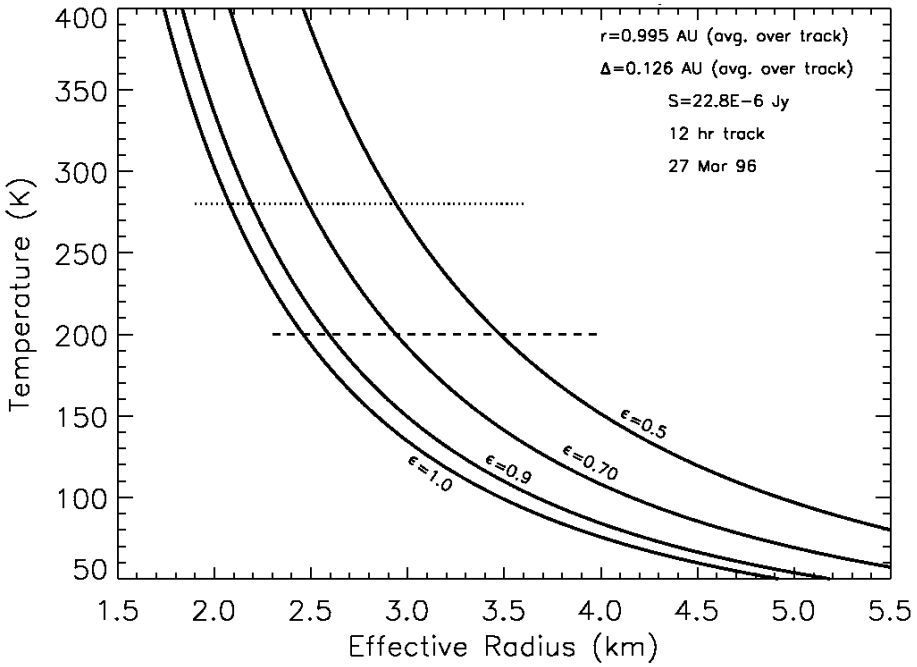

Figure 6.3: Size and temperature of C/1996 B2 nucleus. Here, the loci of points on the temperature-radius parameter plane that can satisfy the upper limit to the microwave flux are displayed. The different curves represent different microwave emissivities.

disruption) would necessarily produce some microwave radiation, but these theories are not yet developed enough to provide a prediction of the microwave flux to compare with our results. However, the derived flatness of the spectrum does rule out synchrotron emission (which typically has a spectral index of 1 to 2) as the source of the X-rays, as would be expected from the typically low strength of the interplanetary magnetic field.

6.3 Optical Measurements

I have described much of this information in a paper first-authored by my colleague (Lisse *et al.* 1999b), and I reproduce much of the text here.

6.3.1 Coma-to-Nucleus Contrast in the Images

The optical data are four nights worth of imaging during 19 to 23 March, 1996, at the KPNO 0.9-m telescope. The sky during three of the nights was photometric or nearly photometric. I used a 2048-by-2048 pixel CCD with a field of view of over 20 arcmin, so I have good maps of the inner coma immediately before the large outburst of activity that coincided with the widely-reported fragmentation of the nucleus (Lecacheux *et al.* 1996, Weaver 1996). The wavelengths I will concentrate on here are at 4845 Å and 6840 Å, the wavelengths of the narrowband continuum in the International Halley Watch filter set. The image scale was $0.68''$ per pixel side. During the run the comet was 0.23 to 0.12 AU from Earth, 1.17 to 1.08 AU from the Sun, and 37° to 42° in phase angle. Typical FWHM of the seeing disk during the photometric and partially photometric time averaged $1.8''$.

Considering the size of the nucleus, the gas and dust output of the comet was extremely prodigious. Whereas most comets have up to just 1% of their nuclear surface area active, Hyakutake seems to be more in the vicinity of 50%, possibly 100% (Lisse *et al.* 1999b). This high fraction is strong evidence for an icy grain halo contributing to the output of water; the total surface area of cometary solids available to release gas is not just the $4\pi R^2$ of the nucleus, but all of the icy grains as well. Moreover the radar experiment (Harmon *et al.* 1997) clearly shows that some of the echo power came from grains moving a few meters per second near the nucleus.

The repercussion of this phenomenon is that our optical images of the comet do not have sufficient spatial resolution to photometrically extract the nucleus. Our coma-fitting technique fails to find a central point-source; the coma is swamping all of the nuclear flux. Not only is this a problem in our KPNO data, where the pixels subtend $0.68''$ on a side, but also in *HST* WFPC2 data, where the pixels subtend only $0.045''$ on a side – or just 3.3 km at the comet during closest approach (Weaver *et al.* 1996).

Shown in Fig. 6.4 is an example of the coma-fitting technique applied to one of our KPNO images. The figure is taken from Lisse *et al.* 1999b and is their Fig. 1. There is clearly a point-source residual, but it is far too bright to be just reflected light from the nucleus, unless, as we mention in the paper, the nucleus has an absurd geometric albedo of about 0.5. It only takes a small amount of dark absorbing material mixed with the ice to reduce the albedo below this value.

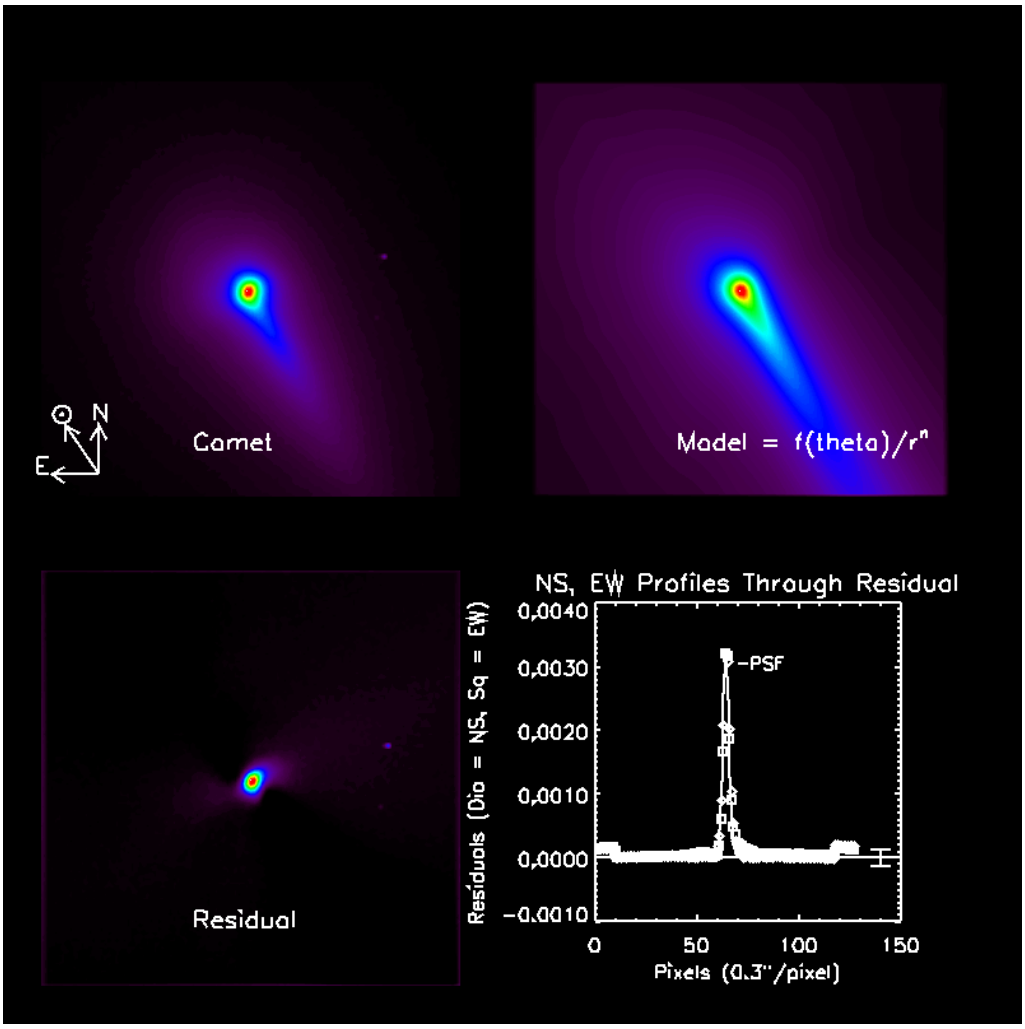

Figure 6.4: Coma-fitting method applied to optical image of Hyakutake. Here I show the results of this image processing technique for Hyakutake. The upper left panel is the original image, the upper right panel is the model, the lower left panel is the difference, and the lower right panel compares the profiles of the residual and the PSF. The residual is point-like but far too bright to be just scattered light from the nucleus. Apparently there was a halo of sublimating icy grains around the nucleus contributing to the optical flux, and the grains were too close to be accounted for in our image processing technique.

6.3.2 Rotation Period

One physical property that we had more success on is the rotation period. Two different methods were used, both the photometric and the morphological methods described in Chapter 3.

Figure 6.5 shows a sequence of narrowband continuum images of the comet over a period of several hours. The overall trend of the coma's brightness – a reciprocal dependence on the cometocentric distance ("$1/\rho$) – has been removed to bring out some of the detail in the coma. Thus it is easier to see when a feature in the coma returns to the same azimuth after one rotation period. The period can be clearly measured as approximately 6 hours, with the caveats mentioned regarding this method in Chapter 3.

A tighter constraint on the period is derived from the photometric data. Figure 6.6 shows the photometry of the comet (nucleus and coma) over 3 nights. The top panel is the absolute flux, the bottom panel has the linear trend removed from the data and an arbitrary sine wave plotted through the points. The data have been scaled in the lower panel to simplify the plotting of this sine wave. The asterisks give the 6840Åflux and the crosses give the 4845Åflux. The circular aperture used for this photometry was 1000 km wide at the comet. The period is quite easily distinguished as 6.3 ± 0.03 hr just by varying the frequency of the sine wave. While this analysis cannot rule out a 12.6-hr period, which would yield a classic double-peaked curve, the coincidence of this period with the morphological evidence in Fig. 6.5 indicates that 6.3 hr and not 12.6 hr is the more tenable choice. The morphological changes and the periodicity are consistent with that found for Hyakutake by Schleicher *et al.* (1998c).

6.4 Summary of Hyakutake Results

The thermal microwave data places a constraint on the nucleus' effective radius of about 3 km. This is consistent with the radar results (Harmon *et al.* 1997) and the mid-IR imaging results (Lisse *et al.* 1999b). Unfortunately, the comet was too active to let us use the coma-fitting method on the optical data to derive the nucleus' optical cross section; this problem even existed for the extreme high resolution *HST* images (Weaver *et al.* 1996). Our only constraint is the geometric albedo of the nucleus is less than 50%.

The rotation period, however, was extractable from the optical data, and combining the photometric and morphological methods, I find a period of 6.3 ± 0.03 hr. The variation in flux within a 1000-km wide aperture was very drastic and mostly due to coma features sweeping in and out of view, not the variation of the nucleus' cross section. The advantage to this is that the period determination became fairly easy. The quoted rotation period has also been widely discovered independently (e.g., Schleicher *et al.* 1998c). The rotation period is toward the low end of known periods, implying that the comet does not have much tensile strength (Lisse *et al.* 1999b).

Figure 6.5: Rotation sequence of comet Hyakutake. This is a sequence of processed optical images of the comet showing the jets sweeping in and out of view over the course of a rotation period. From this it is possible to constrain the rotation period to about 6 hours. The last 2 panels (right side of bottom row) show an original, unprocessed image and the profile of the comet's photocenter, respectively. In the other thirteen panels, the general $1/\rho$ trend of the coma has been removed to help bring out the jet features.

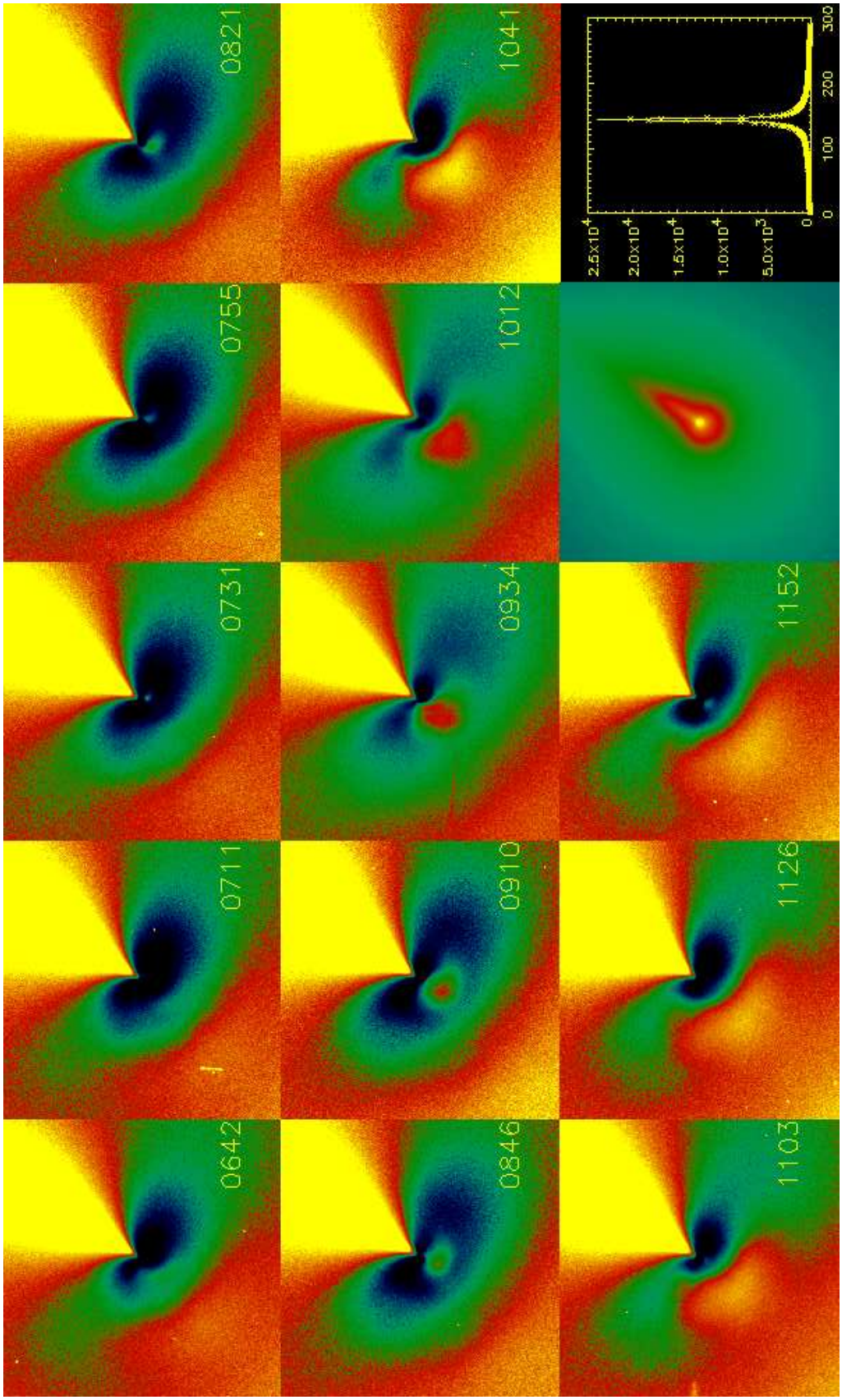
0642
0711
0731
0755
0821
0846
0910
0934
1012
1041
1103
1126
1152
2.5x10^4
2.0x10^4
1.5x10^4
1.0x10^4
5.0x10^3
0
100
200
300

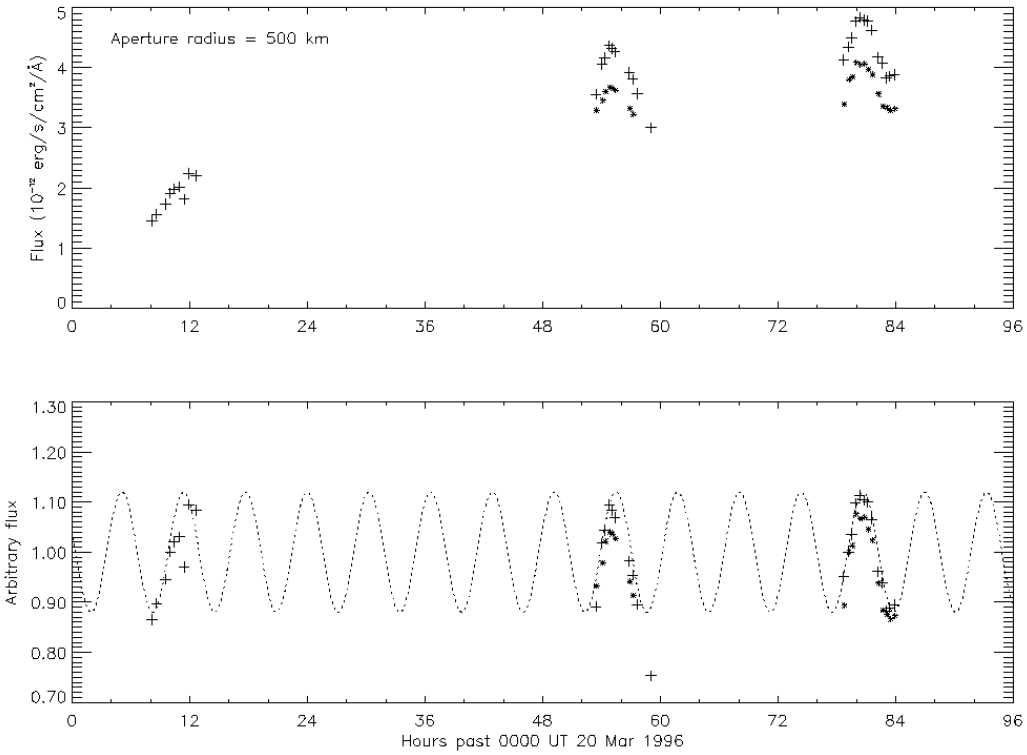

Figure 6.6: Photometry light curve of comet Hyakutake's photocenter. The top panel shows the absolutely calibrated light curve of the comet at two optical wavelengths, over the course of several days. Data from two continuum narrowband filters (4845 Å and 6840 Å) were used. In the bottom panel, a linear trend has been removed, so we can place a sinusoid on top of the light curve to derive a period of about 6.3 hr $\pm$0.05 hr.